APPLIED PHYSICS LETTERS **88**, 061113 (2006)

THz Zenneck surface wave (THz surface plasmon) propagation on a metal sheet

Tae-In Jeon[a] and D. Grischkowsky[b]
School of Electrical and Computer Engineering, Oklahoma State University, Stillwater, Oklahoma 74078

(Received 24 June 2005; accepted 13 December 2005; published online 8 February 2006)

We present an experimental study of the propagation of the THz Zenneck surface wave on an aluminum sheet, now more commonly denoted as the THz surface plasmon (TSP). Here, the TSP pulse is generated by coupling the THz pulse from a metal parallel-plate waveguide onto the aluminum sheet; the propagated TSP pulse is detected at the output end of the sheet using a standard photoconductive dipole antenna. We separate the associated free-space THz pulse from the TSP pulse using a curved sheet. The observed weakly guided TSP propagation has the expected low group velocity dispersion, but also has anomalously high attenuation and much tighter binding to the metal surface than predicted by Zenneck theory. © *2006 American Institute of Physics*.
[DOI: 10.1063/1.2171488]

Surface electromagnetic (EM) waves have now been studied for more than a century, starting with Sommerfeld's study of EM propagation on a single metal wire,[1] and including Zenneck's description of EM propagation on a flat metal surface.[2] An excellent overview of the early EM surface wave investigations is the work by Barlow and Cullen.[3] A more recent work also provides a good description of EM surface wave measurements and experimental techniques.[4] A good description of EM surface waves from the equivalent point of view of surface plasmons is given in Ref. 5. Most recently, the study of surface plasmons has been stimulated by the observation of unusually high transmission resonances through thin metal subwavelength hole arrays at optical frequencies,[6] which have now been studied in the optical, infrared and THz regions.[7]

Here, we describe an experimental study of THz pulses propagating as surface waves, or equivalently as THz surface plasmons (TSP), on a metal sheet. We measure a much higher attenuation of the propagating TSP pulses and a much reduced spatial extent of the TSP evanescent field than predicted by theory. In previous work, such pronounced disagreement between theory and experiment has resulted in a long standing and unresolved controversy.[8–15] It has been experimentally difficult to distinguish between freely propagating EM radiation along the surface and the guided surface wave.[8–15] Due to the collinear propagation and equal phase velocities, power transfer between the two waves easily occurs. Extremely flat and optically smooth surfaces appear to be required to obtain the predicted large propagation distances;[9,12] surface roughness has been predicted to bind the wave more tightly to the surface and thereby increase the attenuation.[12] Submicron layers of high-index, low-loss dielectrics on the metal surface can reduce the extent of the evanescent field by an order of magnitude, causing much higher propagation loss.[10,11,14]

Our experimental study involved measuring TSP propagation on 10-cm-wide by 51-μm-thick Al sheets of different lengths with smooth, but not polished surfaces. As shown in Fig. 1(a), the initially freely propagating THz pulses were collimated and focused into the waveguide by three silicon optics L_1–L_3. The plano-cylindrical lens L_3 produces a line focus on the input air gap between the two Al plates of the parallel plate waveguide, thereby coupling the THz pulses into the waveguide.[16] An extension of the Al sheet is placed in the waveguide on top of the lower plate to efficiently couple onto the Al sheet. For the detection of the propagated TSP pulse, the end of the Al sheet is placed just below the photoconductive dipole antenna, driven by the laser sampling beam. This same detection was used for investigating THz propagation in coaxial cable,[17] and on the single metal wire.[18]

The THz pulses from the waveguide consist of a free-space THz pulse and the TSP pulse coupled to the Al sheet. In order to temporally separate these two THz pulses propagating at c, the Al sheet is curved downward to form a 2-mm-deep curve, as shown in Fig. 1(a). The upper measurement of Fig. 1(b) shows the freely propagating THz pulse overlaying the delayed TSP pulse, which has propagated the full length of the Al sheet, 0.45 mm longer than the line of sight air-space path. In order to block the air-space pulse, a 10-cm-wide Al plate is vertically placed in the middle of the curve to produce a 1.5 mm slit opening between the plate and the curved sheet. The resulting lower pulse of Fig. 1(b) shows only the TSP pulse, with a full width at half maximum (FWHM) pulsewidth of 0.74 ps, and an amplitude spectrum [Fig. 1(d)] peaking at 0.3 THz and extending to 1 THz. Overlapping of the two THz pulses in Fig. 1(c) shows that the 1.5 mm slit removed the air-space pulse without attenuating or distorting the TSP pulse.

We now compare the above slit transmitted TSP pulse observation to the diffraction of an incident plane wave from a similar $z=1.5$-mm-high slit aligned along the y axis on a flat metal surface in the x-y plane at $z=0$, which due to reflection is equivalent to an $h=3$-mm-wide slit in free space. The first null of the equivalent 3 mm single-slit vertical, diffraction pattern occurs at the angle $\sin\theta=\lambda/h$, corresponding to $z=x\tan\theta$ for a propagation distance x from the slit. For $x=8$ cm and $\lambda=1$ mm (0.3 THz), the first null occurs at $z=28.3$ mm, and the half width at half maximum

[a]Permanent address: Division of Electrical and Electronics Engineering, Korea Maritime University, Busan, Korea.
[b]Author to whom correspondence should be addressed; electronic mail: grischd@ceat.okstate.edu

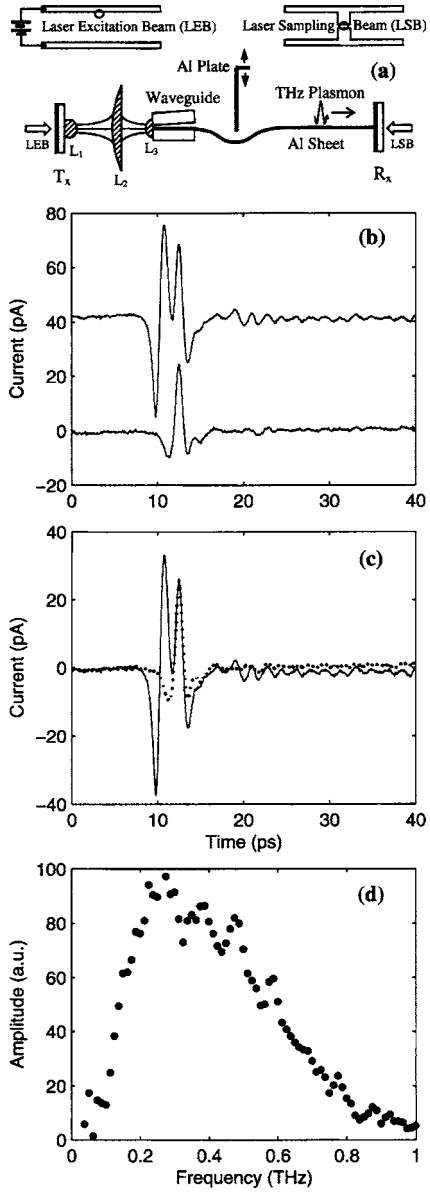

FIG. 1. (a) Schematic diagram of experimental setup. (b) The upper pulses show the separated air-space propagated THz pulse and TSP pulse. The lower pulse shows only the TSP pulse. (c) The overlapping of two pulses in (b). (d) Spectrum of the TSP pulse.

(HWHM) at $z=11.8$ mm. Assuming that the total power transmitted through the 1.5 mm slit is approximately equal to the power in the diffraction pattern from $z=0$ to the HWHM at $z=11.8$ mm, the diffracted intensity would be reduced by the ratio $(1.5\ \text{mm}/11.8\ \text{mm})=0.13$, corresponding to the amplitude reduction factor 0.36. However, no reduction of the TSP pulse was observed, thereby indicating the tight binding to the curved surface.

To study the transmission of the TSP pulse through the short air gap shown in Fig. 2, the curve depth was increased to 4 mm, and the Al blocking plate was removed. Figure 2 shows both the measured free-space THz pulse and the associated TSP pulse for the different air-gap separations G. The peak-to-peak ratios of the air transmitted TSP pulses are reduced only by 6% and 14%, for G=1.1 and 5.6 mm, respectively, compared to G=0. The amplitude transmission of 94% for G=1.1 mm indicates the relatively small 35% reflection at the air gap, due to the weak guiding and easy coupling of the TSP pulse into freely propagating radiation.

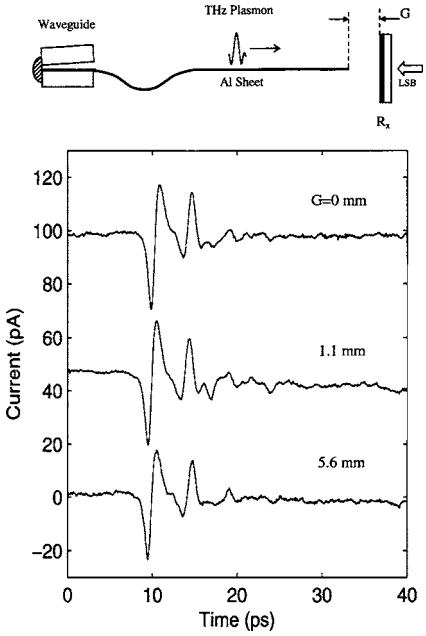

FIG. 2. Measured THz pulses for the air-gaps G. The upper figure shows the experimental setup.

Figure 3 shows a comparison between long air-gap and long Al sheet propagation. Al sheet I has a 2 mm curve depth with the blocking plate set for a $Z_I=1.5$ mm opening, and the total distance from input waveguide to receiver is 98 cm, including the 84 cm air gap. The measured peak-to-peak amplitude of the TSP pulse transmitted through the air gap is 3.0 pA, which is 9% of the corresponding 34 pA TSP pulse for the shorter 14-cm-long continuous Al sheet in Fig. 1. However, when Al sheet II is put over the air gap to produce an effectively continuous sheet, the measured peak-to-peak TSP pulse amplitude increases to 5.1 pA. In this case the FWHM pulsewidth is 0.76 ps, indicating low group velocity dispersion. Considering that the peak-to-peak TSP pulse attenuates from 34 to 5.1 pA due to the additional 84 cm Al sheet II propagation, indicates an effective amplitude attenuation coefficient of $\alpha=0.023\ \text{cm}^{-1}$. This value is only an upper limit, because the TSP beam spreading has been neglected.

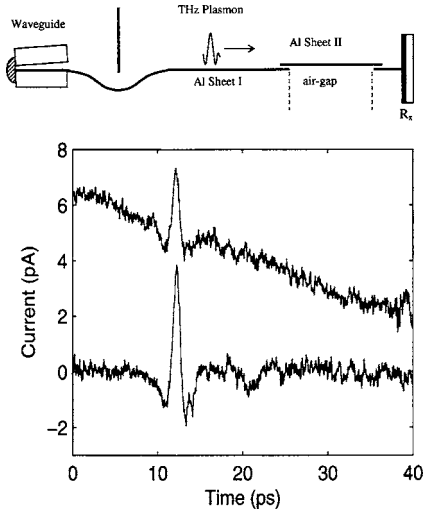

FIG. 3. Comparison of air propagated (upper pulse) and Al sheet II propagated (lower pulse) TSP. The upper figure shows the experimental setup.

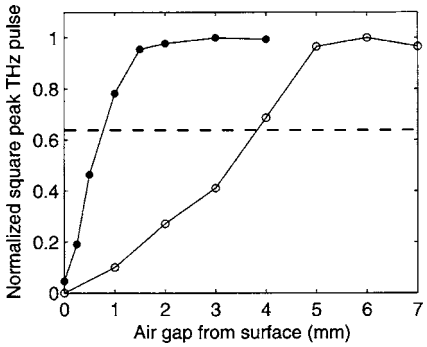

FIG. 4. Normalized measurements of the square of the peak TSP pulse amplitude vs slit opening Z_I at the center of the 6-mm-deep curve (dots), and the square of the peak TSP pulse amplitude vs slit opening Z_{II} at the center of the 15.7-cm-long Al sheet II (open circles).

We also measured the extent of the evanescent field of the propagating TSP pulses using the setup of Fig. 1(a) with a curve depth of 6 mm. The peak amplitude of the well separated TSP pulses was measured as a function of the slit width Z_I between the Al blocking plate and the curved sheet. Because field falls off vertically from the surface as $\exp[-\beta_I z]$, the normalized transmitted power is given by $[1-\exp(-2\beta_I Z_I)]$. Consequently, the normalized square of our measurements shown by the dots in Fig. 4 can determine β_I. For the normalized curve to equal $(1-1/e)$, shown as the horizontal dashed line, the value of $Z_I=1/(2\beta_I)$ is approximately 0.8 mm. Thereby, $\beta_I=6.25\ \mathrm{cm}^{-1}$ and $L_{\beta I}=1/\beta_I=1.6$ mm, consistent with the results of Fig. 1, and indicating a well attached TSP pulse propagating around the curve.

This same type of measurement was repeated with a setup similar to Fig. 3, but with a shorter Al sheet II covering an air gap of 15.7 cm, and a second Al blocking plate vertically installed above the center of the covered air gap. The distance between the input waveguide to the receiver was 29.7 cm. Again, the peak amplitude of the propagated TSP pulses was measured as a function of the slit width Z_{II} between the second blocking plate and Al sheet II. The square of these amplitude measurements is shown as the open circles in Fig. 4, where $Z_{II}=3.8$ mm at the value $(1-1/e)$, giving $\beta_{II}=1.32\ \mathrm{cm}^{-1}$, and $L_{\beta II}=7.6$ mm, indicating a much larger extent of the evanescent field of the TSP pulse for the straight sheet compared to the curved sheet.

For the diffraction of a freely propagating THz pulse incident on the slit, the diffracted pulse amplitude squared would increase quadratically with Z_{II}, because the total power through the slit would increase linearly with Z_{II} and the angular divergence would decrease as $1/Z_{II}$. The observed increase is much slower than a quadratic response, again indicating the guided nature of the surface wave.

Zenneck surface wave theory[2–4] and surface plasmon theory,[5,19] are equivalent for TSP pulse propagation on a metal sheet as $\exp[ikx]$ with the propagation constant $k=k_r+ik_i$. For our Al sheet we assume the handbook value of dc conductivity $\sigma_0=3.54\times10^5/(\Omega\,\mathrm{cm})$, and at 0.4 THz obtain the complex dielectric constant from Drude theory as $\varepsilon=\varepsilon_r+i\varepsilon_i=-3.3\times10^4+i1.6\times10^6$.[20,21] For this case $k_r=k_0=2\pi/\lambda_0$ to an accuracy of 1 part in 10^5, where λ_0 is the free-space wavelength, and the relationship for $k_i=\alpha$ simplifies to $\alpha=k_0/(2\varepsilon_i)$. At 0.4 THz we obtain the extremely small value $\alpha=0.000\,026\ \mathrm{cm}^{-1}$, corresponding to the very large, surface-wave propagation length of $L_\alpha=1/\alpha=38\,500$ cm, 900 times larger than experiment ($L_\alpha=43.5$ cm). For our case, $\beta=[2k_rk_i\exp(i\pi/2)]^{1/2}$, which simplifies to $\beta=[k_0(2\varepsilon_i)^{-1/2}][1+i]\equiv\beta_0(1+i)$. At 0.4 THz, we obtain $\beta_0=0.047\ \mathrm{cm}^{-1}$ giving the evanescent field $1/e$ falloff $L_\beta=21.5$ cm, 28 times larger than experiment $L_{\beta II}=7.6$ mm. The self-consistent relationship $\alpha=\beta_0^2/k_0$ requires that the observed factor of 28 increase in β_0 causes a corresponding factor of 790 increase in $\alpha=0.021\ \mathrm{cm}^{-1}$, in good agreement with the measurement of $\alpha=0.023\ \mathrm{cm}^{-1}$.

A possible resolution of the large discrepancy between theory and experiment is based on the situation that the "true" Zenneck wave is difficult to establish, because of its large spatial extent $L_\beta=21.5$ cm. An initial propagation distance much larger than L_β would be required for the evolving guided surface wave (with smaller extent and higher absorption) to expand to the size of the stable Zenneck wave with the corresponding 1/900 reduced loss given by $\alpha=\beta_0^2/k_0$.

The authors thank Jiangquan Zhang for illuminating discussions, Adam Bingham and Sarika Pokharel for important comments on the manuscript, and Darpan Pradhan for experimental assistance. This work was partially supported by the National Science Foundation.

[1] A. Sommerfeld, Ann. Phys. Chem. **67**, 233 (1899).
[2] J. Zenneck, Ann. Phys. **23**, 846 (1907).
[3] H. M. Barlow and A. L. Cullen, Proc. IEE **100**, 329 (1953).
[4] G. N. Zhizhin, M. A. Moskalova, E. V. Shomina, and V. A. Yakovlev, in *Surface Polaritons*, edited by V. M. Agranovich and D. L. Mills (North-Holland, Amsterdam, 1982).
[5] H. Raether, *Surface Plasmons on Smooth and Rough Surfaces and on Gratings* (Springer, Berlin, 1988).
[6] T. W. Ebbesen, H. J. Lezec, H. F. Ghaemi, T. Thio, and P. Q. Wolff, Nature (London) **391**, 667 (1998).
[7] W. L. Barnes, A. Dereux, and T. W. Ebbesen, Nature (London) **424**, 824 (2003).
[8] D. L. Begley, R. W. Alexander, C. A. Ward, R. Miller, and R. J. Bell, Surf. Sci. **81**, 245 (1979).
[9] E. S. Koteles and W. H. McNeill, Int. J. Infrared Millim. Waves **2**, 361 (1981).
[10] Z. Schlesinger and A. J. Sievers, Phys. Rev. B **26**, 6444 (1982).
[11] K. W. Steijn, R. J. Seymour, and G. I. Stegeman, Appl. Phys. Lett. **49**, 1151 (1986).
[12] D. L. Mills and A. A. Maradudin, Phys. Rev. B **39**, 1569 (1989).
[13] M. Klopfleisch and U. Schellenberger, J. Appl. Phys. **70**, 930 (1991).
[14] J. Saxler, J. Gomerz Rivas, C. Janke, H. P. M. Pellemans, P. Haring Bolivar, and H. Kurz, Phys. Rev. B **69**, 155427 (2004).
[15] J. F. O'Hara, R. D. Averitt, and A. J. Taylor, Opt. Express **13**, 6117 (2005).
[16] R. Mendis and D. Grischkowsky, Opt. Lett. **26**, 846 (2001).
[17] T.-I. Jeon and D. Grischkowsky, Appl. Phys. Lett. **85**, 6092 (2004).
[18] T.-I. Jeon, J. Zhang, and D. Grischkowsky, Appl. Phys. Lett. **86**, 161904 (2005).
[19] F. Yang, J. R. Sambles, and G. W. Bradberry, Phys. Rev. B **44**, 5855 (1991).
[20] D. Qu, D. Grischkowsky, and W. Zhang, Opt. Lett. **29**, 896 (2004).
[21] D. Qu and D. Grischkowsky, Phys. Rev. Lett. **93**, 196804 (2004).